mTOR complex 2 in adipose tissue negatively controls whole-body growth

Nadine Cybulski[a,1], Pazit Polak[a,1], Johan Auwerx[b,2], Markus A. Rüegg[a], and Michael N. Hall[a,3]

[a]Biozentrum, University of Basel, 4056 Basel, Switzerland; and [b]Institut de Génétique et de Biologie Moléculaire et Cellulaire and Institut Clinique de la Souris, CNRS/INSERM/Université Louis Pasteur, 67404 Illkirch, France

Edited by Craig B. Thompson, University of Pennsylvania, Philadelphia, PA, and approved April 27, 2009 (received for review November 10, 2008)

Mammalian target of rapamycin (mTOR), a highly conserved protein kinase that controls cell growth and metabolism in response to nutrients and growth factors, is found in 2 structurally and functionally distinct multiprotein complexes termed mTOR complex 1 (mTORC1) and mTORC2. mTORC2, which consists of rictor, mSIN1, mLST8, and mTOR, is activated by insulin/IGF1 and phosphorylates Ser-473 in the hydrophobic motif of Akt/PKB. Though the role of mTOR in single cells is relatively well characterized, the role of mTOR signaling in specific tissues and how this may contribute to overall body growth is poorly understood. To examine the role of mTORC2 in an individual tissue, we generated adipose-specific *rictor* knockout mice (*rictor*$^{ad-/-}$). *Rictor*$^{ad-/-}$ mice are increased in body size due to an increase in size of nonadipose organs, including heart, kidney, spleen, and bone. Furthermore, *rictor*$^{ad-/-}$ mice have a disproportionately enlarged pancreas and are hyperinsulinemic, but glucose tolerant, and display elevated levels of insulin-like growth factor 1 (IGF1) and IGF1 binding protein 3 (IGFBP3). These effects are observed in mice on either a high-fat or a normal diet, but are generally more pronounced in mice on a high-fat diet. Our findings suggest that adipose tissue, in particular mTORC2 in adipose tissue, plays an unexpectedly central role in controlling whole-body growth.

genetics | mTORC2 | signal transduction | rapamycin

Mammalian target of rapamycin (mTOR), a highly conserved protein kinase that controls cell growth and metabolism in response to nutrients and growth factors, is found in 2 structurally and functionally distinct multiprotein complexes termed mTOR complex 1 (mTORC1) and mTORC2 (1). mTORC1 contains raptor, mLST8, PRAS40, and mTOR, and is sensitive to the immunosuppressant and anticancer drug rapamycin (2–5). mTORC2 consists of rictor, mSIN1, mLST8, and mTOR, and is insensitive to rapamycin, although long-term rapamycin treatment can indirectly inhibit mTORC2 in some cell types (6–10). The best-characterized substrates of mTOR are S6K and 4E-BP, via which mTORC1 controls translation, and Akt/PKB, via which mTORC2 may control cell survival and possibly other processes (11–13). mTORC2 also phosphorylates and activates SGK1, and phosphorylates and stabilizes PKCα (8, 14–16). As mTORC1 can be pharmacologically inhibited with rapamycin, it is relatively well characterized and has been implicated in various disorders, including cancer, cardiovascular disease, obesity, and diabetes (1). In contrast, as there is no specific inhibitor of mTORC2, mTORC2 signaling is less well characterized and its physiological role is unclear. Knockout studies have underscored the importance of both complexes, as full-body deletion of any component of either mTOR complex results in embryonic lethality (6, 10, 17, 18). *Rictor*-deficient embryos fail to develop beyond day E10.5 and arrest as slightly smaller and developmentally delayed embryos compared with littermate controls (17, 18).

Though the general role of mTOR in single cells is relatively well characterized, the role of mTOR signaling in specific tissues and how this may contribute to overall body growth and whole-body metabolism is poorly understood (11). Adipose-specific *raptor* knockout mice are resistant to diet-induced obesity and have improved glucose metabolism (19). Conditional knockout of *raptor* in skeletal muscle results in slight glucose intolerance, muscle dystrophy, and death by the age of 6 months (20). Knockout of *rictor* specifically in skeletal muscle results in little to no phenotype and thus provided little insight on the physiological role of mTORC2, at least in muscle (20, 21).

Adipose tissue is a fat storage depot and an endocrine organ that controls energy metabolism, appetite, and fertility in response to nutrients and insulin (22, 23). Interestingly, the equivalent tissue in *Drosophila*, the fat body, controls full-body growth in response to nutrients. Colombani et al. (24) have shown that downregulation of TOR signaling, most likely mTORC1, specifically in the fat body, results in a reduction in overall body size. Excess adipose tissue (obesity) leads to many metabolic disorders, including type 2 diabetes, cardiovascular diseases, and cancer. Given the central role of mTOR as a nutrient sensor and the increasing prevalence of obesity, it is important to understand the role of adipose mTOR in controlling whole-body growth and metabolism. In this study, we examined the role of mTORC2 in adipose tissue. To circumvent the embryonic lethality caused by full-body ablation of any component of mTORC2, we used the Cre/LoxP system to knock out *rictor* specifically in adipose tissue. Strikingly, *rictor*$^{ad-/-}$ mice are enlarged due to an increase in lean tissue mass resulting from elevated levels of IGF1. Furthermore, the knockout mice are hyperinsulinemic yet glucose tolerant. These findings suggest the existence of an mTORC2-dependent adipose to liver/pancreas signaling axis that controls full-body growth and metabolism.

Results

Generation and Confirmation of Adipose-Specific *rictor* Knockout Mice. To delete *rictor* in adipose tissue, we generated mice in which exons 4 and 5 of the *rictor* gene were flanked by *loxP* sites (*rictor*$^{fl/fl}$). The *rictor*$^{fl/fl}$ mice were crossed with mice expressing cre recombinase under control of the adipose-specific, *fabp4*/*aP2* gene promoter (25) (Fig. 1*A*). Adipose-specific *rictor* knockout mice (*rictor*$^{ad-/-}$) lacked rictor protein in adipose tissue but not in liver, heart, kidney, spleen, brain, or macrophages (Fig. 1*B* and Fig. S1), indicating that *rictor* was indeed deleted specifically in adipocytes. Adipose tissue of *rictor*$^{ad-/-}$ mice exhibited reduced Akt Ser-473 phosphorylation and reduced PKCα levels, indicating that mTORC2 signaling was defective (Fig. 1*B*). As expected, Akt Thr-308 phosphorylation and phosphorylation of the Akt substrate GSK3 was not affected in adipose tissue.

***Rictor*$^{ad-/-}$ Mice Are Enlarged Due to an Increase in Lean Mass.** Body weight of *rictor*$^{ad-/-}$ and control wild-type littermates (*rictor*$^{fl/fl}$) was

Author contributions: N.C., P.P., M.A.R., and M.N.H. designed research; N.C., P.P., and J.A. performed research; N.C., P.P., J.A., M.A.R., and M.N.H. analyzed data; and N.C. and M.N.H. wrote the paper.

The authors declare no conflict of interest.

This article is a PNAS Direct Submission.

[1]N.C. and P.P. contributed equally to this work.

[2]Present address: École Polytechnique Fédérale de Lausanne, 1015 Lausanne, Switzerland

[3]To whom correspondence should be addressed. E-mail: m.hall@unibas.ch.

This article contains supporting information online at www.pnas.org/cgi/content/full/0811321106/DCSupplemental.

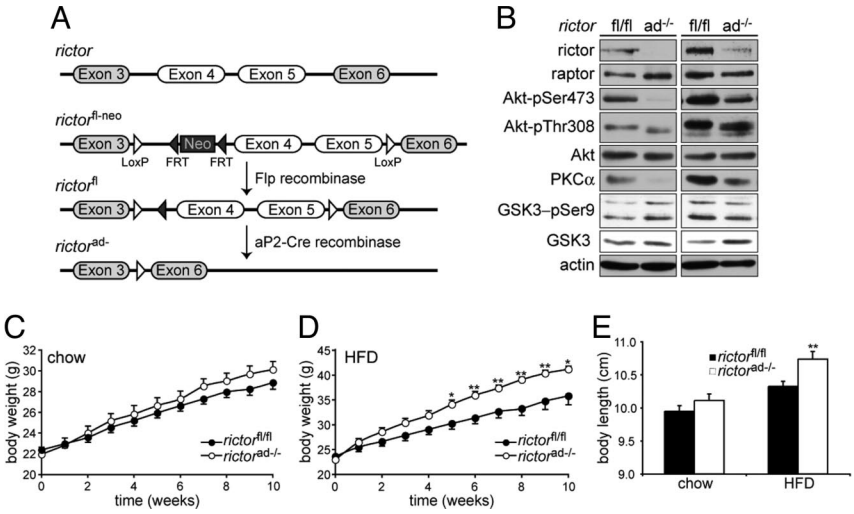

Fig. 1. Adipose-specific *rictor* knockout mice have increased body weight. (*A*) Adipose-specific *rictor* knockout mice (*rictor*$^{ad-/-}$) were generated using the Cre/LoxP system (see *Methods*). (*B*) Immunoblot showing knockout of *rictor* and impaired mTORC2 signaling in adipose tissue of 2 littermates. A short (*Right*) and long (*Left*) exposure are shown. Residual rictor protein in *rictor*$^{ad-/-}$ in the long exposure is likely from stromal vascular cells in the adipose tissue that do not express aP2-Cre. (*C*) Weight curves of *rictor*$^{fl/fl}$ ($n = 16$) and *rictor*$^{ad-/-}$ ($n = 14$) male mice 8–18 weeks of age maintained on a chow diet. (*D*) Weight curves of *rictor*$^{fl/fl}$ and *rictor*$^{ad-/-}$ male mice fed an HFD for 10 weeks ($n = 10$ per genotype). (*E*) Body length determined by measuring nasal-to-anal distance. Mice were put on an HFD at the age of 8 weeks. Values in *C–E* are mean ± SEM. $*P < 0.05$; $**P < 0.01$, *rictor*$^{ad-/-}$ vs. *rictor*$^{fl/fl}$.

monitored during a 10-week time course in mice 8–18 weeks of age. At 8 weeks of age, knockout and control mice were of similar weight. On a normal diet (chow), *rictor*$^{ad-/-}$ mice gained weight at a slightly higher rate than control mice such that they were 4% heavier at the end of the time course (Fig. 1*C*). The increased body weight of *rictor*$^{ad-/-}$ mice compared with control mice was more pronounced on an HFD (Fig. 1*D*). After 10 weeks on an HFD (started at 8 weeks of age), the *rictor*$^{ad-/-}$ mice were 17% heavier than control *rictor*$^{fl/fl}$ mice, but were already significantly heavier after only 5–6 weeks on the HFD. Body length of the *rictor*$^{ad-/-}$ mice was also increased (Fig. 1*E*), suggesting that the increase in weight was due to an overall increase in body size rather than an increase only in fat mass. Indeed, whole-body dexa scan analysis of mice after 6 weeks on an HFD revealed an increase specifically in lean tissue mass (Fig. 2*A*); no difference was observed in the total amount of fat mass after 6 weeks on an HFD (Fig. 2*B*).

To investigate further the increase specifically in lean tissue mass, individual organs of *rictor*$^{ad-/-}$ and *rictor*$^{fl/fl}$ mice, fed either a chow or HFD for 10 weeks, were excised and weighed (Fig. 2 *C–J*). On a chow diet, the heart, kidneys, spleen, and pancreas were 40%, 28%, 38%, and 41% heavier, respectively, in *rictor*$^{ad-/-}$ mice compared with *rictor*$^{fl/fl}$ control mice. On an HFD, the heart, kidneys, spleen, and pancreas were 40%, 47%, 62%, and 129% heavier, respectively, in *rictor*$^{ad-/-}$ mice (Fig. 2 *C–F*). Interestingly, the pancreas was heavier in the *rictor*$^{ad-/-}$ mice on both diets but was disproportionately heavier (129%) on the HFD, compared with other organs (Fig. 2*F*). The liver was also heavier (75%) in *rictor*$^{ad-/-}$ mice, but only on the HFD (Fig. 2*G*). Furthermore, as revealed by whole-body dexa scan analysis, *rictor*$^{ad-/-}$ mice exhibited a 15% increase in bone mineral content with no change in bone mineral density, indicating that overall bone size was also increased (Fig. 2*H*). Thus, all lean tissues examined were enlarged as a result of an mTORC2 deficiency in adipose tissue.

After 10 weeks on an HFD, the inguinal fat pad was not significantly increased in *rictor*$^{ad-/-}$ mice compared with control *rictor*$^{fl/fl}$ mice (Fig. 2*I*), although the epididymal fat pad was increased 30% (Fig. 2*J*). This is consistent with the dexa scan analysis described above that detected no increase in overall fat mass after 6 weeks on an HFD. Thus, *rictor*$^{ad-/-}$ mice are larger than control mice due to an increase mainly, if not exclusively, in lean tissue mass. Surprisingly, this effect was particularly evident in mice on an HFD. Furthermore, given the increase in lean mass with little to no increase in overall fat mass, *rictor*$^{ad-/-}$ mice are leaner than control mice. This leanness could account for the relatively mild increase in full-body weight (17%) compared with the observed increases in weights of individual organs.

***Rictor*$^{ad-/-}$ Mice Exhibit Normal Adipose Tissue Morphology and Have Increased Liver Steatosis.** To investigate further the effect of *rictor*$^{ad-/-}$ on adipose tissue, we performed histology on the epi-

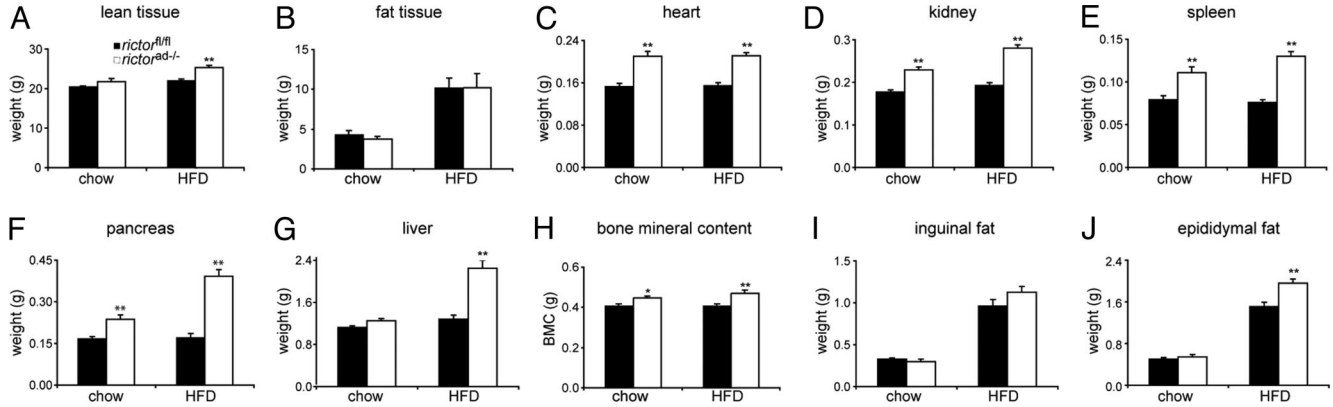

Fig. 2. *Rictor*$^{ad-/-}$ mice have increased lean mass. (*A* and *B*) Lean mass (*A*) and fat mass (*B*) in *rictor*$^{fl/fl}$ and *rictor*$^{ad-/-}$ mice was determined by dexa scan analysis. Mice were maintained on a chow diet or HFD for 6 weeks ($n = 6–8$ per group). (*C–J*) Weight of individual organs. Individual organs were excised and weighed. Mice were maintained on a chow diet or HFD for 10 weeks. Bone mineral content was determined by dexa scan analysis as in *A* and *B*. Values in *A–J* are represented as mean ± SEM ($n = 11–27$ per genotype; $n = 5$ in *F*). $*P < 0.05$; $**P < 0.01$, *rictor*$^{ad-/-}$ vs. *rictor*$^{fl/fl}$.

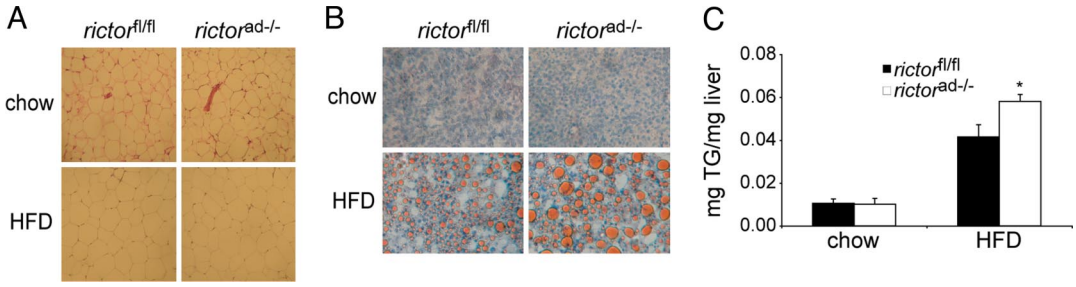

Fig. 3. *Rictor*$^{ad-/-}$ mice have unaltered adipose tissue morphology and increased hepatic steatosis. (*A*) Representative image of H&E stained sections of epididymal fat. (*B*) *Rictor*$^{ad-/-}$ and *rictor*$^{fl/fl}$ develop hepatic steatosis after HFD. Representative image of liver sections stained with Oil Red O and hematoxylin. (*C*) Quantification of liver triglycerides in mice fed a chow diet ($n = 4$ per group) or an HFD for 10 weeks ($n = 16$ per group).

didymal fat pad. The epididymal fat pads from *rictor*$^{ad-/-}$ and control *rictor*$^{fl/fl}$ mice were indistinguishable with regard to fat cell size and morphology (Fig. 3*A*). We also examined histological sections of the liver, a secondary fat storage organ. Hepatic cells from HFD-fed *rictor*$^{ad-/-}$ mice contained particularly enlarged lipid droplets, indicative of more advanced steatosis (Fig. 3*B*). Quantification of liver triglycerides confirmed the increased fat accumulation in the liver of *rictor*$^{ad-/-}$ mice compared with control *rictor*$^{fl/fl}$ mice (Fig. 3*C*). The amount of glycogen in the liver was not changed in *rictor*$^{ad-/-}$ mice compared with control mice (supporting information (SI) Fig. S2). Thus, the increase in hepatic fat accumulation likely accounts for the particularly enhanced size (75% increase) of the liver in HFD-fed *rictor*$^{ad-/-}$ mice, as described previously.

***Rictor*$^{ad-/-}$ Mice Have Altered Levels of Cholesterol and Adiponectin.** To characterize further the phenotype of *rictor*$^{ad-/-}$ mice, we examined several blood metabolites and hormones that could be affected upon altered adipose function. Free fatty acids and triglyceride levels were unchanged in *rictor*$^{ad-/-}$ mice compared with *rictor*$^{fl/fl}$ mice. Cholesterol levels were increased in *rictor*$^{ad-/-}$ mice, but only on a chow diet. Serum leptin and IL-6 were also unchanged, but serum levels of adiponectin were decreased ≈30% in *rictor*$^{ad-/-}$ mice, on either a chow or high-fat diet (Table 1).

***Rictor*$^{ad-/-}$ Mice Are Hyperinsulinemic but Glucose Tolerant.** To assess the role of adipose mTORC2 in whole-body glucose metabolism, we first examined blood glucose and insulin levels. On a chow or high-fat diet, blood glucose levels were similar or slightly lower in both fasted (overnight) and fed *rictor*$^{ad-/-}$ mice compared with control *rictor*$^{fl/fl}$ mice (Fig. 4 *A* and *B*). However, insulin levels were significantly increased in fasted or fed *rictor*$^{ad-/-}$ mice compared with control mice, on a chow or high-fat diet (Fig. 4 *C* and *D*). To further investigate the effect of mTORC2-deficient adipose tissue on insulin levels, we performed a morphometric analysis on the pancreas. Consistent with an enlarged pancreas, pancreatic islets were at least 2-fold larger but otherwise morphologically unchanged in *rictor*$^{ad-/-}$ mice compared with control *rictor*$^{fl/fl}$ mice (Fig. 4 *E* and *F*). Furthermore, the increase in size of the islets correlated with an increase in total weight of β cells (Fig. 4*G*). The increase in size of the pancreas and insulin-producing islets, even disproportionately increased in HFD-fed knockout mice, likely account for the hyperinsulinemia of *rictor*$^{ad-/-}$ mice.

We next performed a glucose tolerance test on *rictor*$^{ad-/-}$ and control *rictor*$^{fl/fl}$ mice, on a chow or high-fat diet. Hyperinsulinemia, as observed in the *rictor*$^{ad-/-}$ mice, is normally a response to insulin resistance and generally correlates with glucose intolerance. However, unexpectedly, the hyperinsulinemic *rictor*$^{ad-/-}$ mice were similarly glucose tolerant (chow diet) or even more glucose tolerant (HFD) than *rictor*$^{fl/fl}$ mice on the corresponding diets (Fig. 5 *A* and *B*). Furthermore, *rictor*$^{ad-/-}$ mice produced higher levels of blood insulin in response to an injected glucose bolus, compared with *rictor*$^{fl/fl}$ control mice (Fig. S3). Thus, *rictor*$^{ad-/-}$ mice remain glucose tolerant under conditions (HFD) where wild-type mice are unable to do so. In addition, the hyperinsulinemia of *rictor*$^{ad-/-}$ mice does not correlate with glucose intolerance but may rather reflect a primary effect of mTORC2-deficient adipose on the pancreas. Such a primary effect on the pancreas could underlie the disproportionately large size of the pancreas in *rictor*$^{ad-/-}$ mice.

rictor$^{ad-/-}$ mice are more glucose tolerant than control mice. Is this due to increased insulin sensitivity, to the observed elevated levels of insulin, or to both? To distinguish these possibilities, we examined the insulin sensitivity of *rictor*$^{ad-/-}$ and *rictor*$^{fl/fl}$ mice. *Rictor*$^{ad-/-}$ mice were slightly insulin resistant compared with the wild-type control mice, based on less efficient clearance of blood glucose in response to injected insulin (Fig. 5*C*). To investigate further this insulin resistance, we examined Akt Thr-308 and Ser-473 phosphorylation in muscle, adipose tissue, and liver of insulin-injected *rictor*$^{ad-/-}$ and *rictor*$^{fl/fl}$ mice. Mice were injected with either saline or insulin and, after 15 min, tissues were excised and processed for immunoblotting to detect Akt phosphorylation. Insulin stimulated Thr-308 and Ser-473 phosphorylation in both the *rictor*$^{ad-/-}$ and control *rictor*$^{fl/fl}$ mice in all 3 tissues, but this stimulation was less robust in the *rictor*$^{ad-/-}$ mice (Fig. 5*D*).

Table 1. Blood metabolites of *rictor*$^{fl/fl}$ and *rictor*$^{ad-/-}$ fed a chow or HFD diet

	chow		HFD	
	rictor$^{fl/fl}$	*rictor*$^{ad-/-}$	*rictor*$^{fl/fl}$	*rictor*$^{ad-/-}$
Cholesterol (mg/dL)	52.1 (2.7)	88.5 (5.9)**	132.0 (6.8)	141.3 (19.8)
Triglycerides (mg/dL)	88.0 (5.1)	93.5 (7.5)	68.7 (3.4)	69.0 (5.3)
Free fatty acids (mM)	0.363 (0.039)	0.402 (0.026)	0.413 (0.042)	0.476 (0.035)
Adiponectin (μg/mL)	59.0 (2.2)	41.6 (2.5)**	60.1 (3.9)	40.0 (2.2)**
Leptin (ng/mL)	5.67 (0.87)	4.6 (0.64)	27.37 (3.44)	25.64 (1.79)
IL-6 (pg/mL)	1.95 (0.90)	1.47 (0.58)	2.63 (0.58)	3.58 (0.82)

Clinical chemistry and hormone values of mice fed a chow diet or HFD for 10 weeks. Values are mean ± SEM ($n = 9$–10 per group). *$P < 0.05$, **$P < 0.01$.

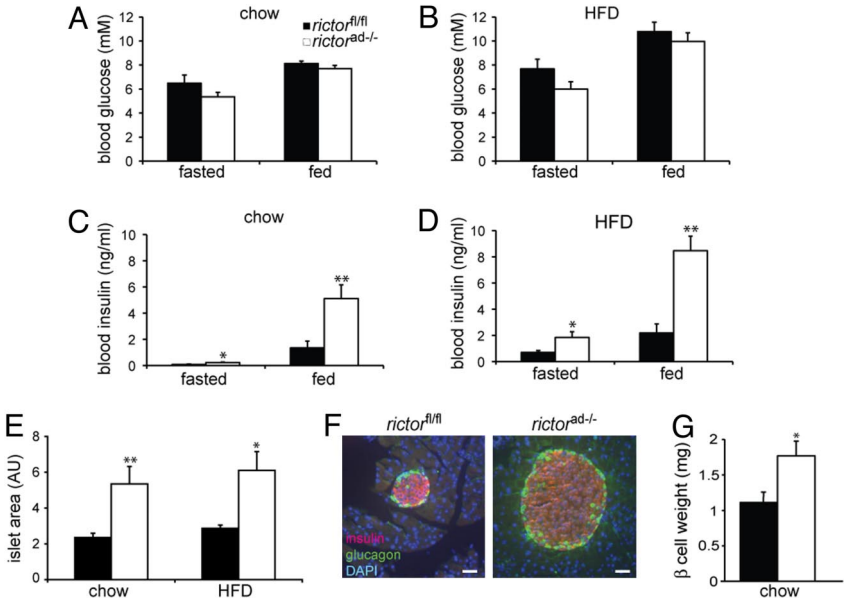

Fig. 4. *Rictor*$^{ad-/-}$ mice are hyperinsulinemic. (*A* and *B*) Blood glucose from overnight fasted or fed mice on either a chow diet (*A*) or HFD for 10 weeks (*B*) ($n = 10–15$). (*C* and *D*) Blood insulin from overnight fasted or fed mice on either a chow diet (*C*) or HFD for 10 weeks (*D*) ($n = 10$). (*E*) Quantification of average islet area represented in arbitrary units (AU). $n = 3–5$ per group. (*F*) Representative image of an islet in *rictor*$^{fl/fl}$ and *rictor*$^{ad-/-}$ mice immunostained for insulin (red) and glucagon (green). Nuclei were stained with DAPI (blue). Images were taken at the same magnification, and islets are shown at the same scale. (*G*) Quantitative analysis of β-cell mass of *rictor*$^{fl/fl}$ and *rictor*$^{ad-/-}$ mice on chow diet.

Thus, *rictor*$^{ad-/-}$ mice are modestly insulin resistant, possibly due to reduced levels of the insulin-sensitizer adiponectin (Table 1). Furthermore, these findings suggest that the glucose tolerance of *rictor*$^{ad-/-}$ mice is due to an elevated level of insulin that overcomes a weak insulin resistance. Elevated levels of IGF1 (see below) might also contribute to the glucose tolerance of *rictor*$^{ad-/-}$ mice (26).

As expected, insulin failed to stimulate mTORC2-dependent Akt Ser-473 phosphorylation in adipose tissue of *rictor*$^{ad-/-}$ mice (Fig. 5*D*). However, insulin stimulated Akt Thr-308 and GSK3 phosphorylation in adipose tissue of *rictor*$^{ad-/-}$ mice, suggesting that mTORC2-deficient adipose tissue remains insulin responsive. To further investigate the insulin responsiveness of mTORC2-deficient adipose tissue, we assayed glucose uptake in isolated, insulin-treated adipocytes. Though basal and insulin-stimulated glucose uptake were lower in *rictor*-deficient adipocytes, both *rictor*$^{ad-/-}$ and wild-type adipocytes displayed a 3-fold stimulation in response to insulin (Fig. 5*E*), confirming that mTORC2-deficient adipocytes remain insulin responsive.

***Rictor*$^{ad-/-}$ Mice Have Elevated Serum IGF1.** Organismal growth is controlled largely by growth hormone (GH) and IGF1 (27, 28). GH

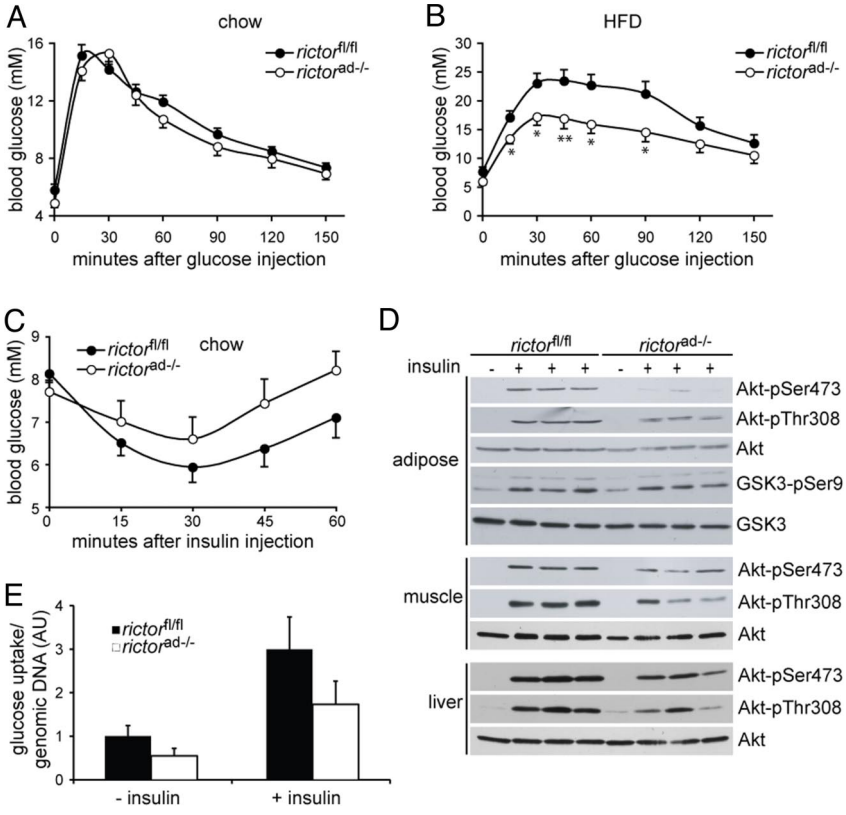

Fig. 5. *Rictor*$^{ad-/-}$ mice have improved glucose tolerance after HFD. (*A* and *B*) Glucose tolerance tests in overnight-starved mice fed a chow diet (*A*) or an HFD for 10 weeks (*B*). Mice were injected with glucose (2 g/kg, i.p.), and blood glucose was subsequently measured at the indicated time points ($n = 10–16$). $*P < 0.05$, $**P < 0.01$, *rictor*$^{ad-/-}$ vs. *rictor*$^{fl/fl}$. $n = 9–10$ per group. (*C*) Insulin sensitivity test in fed mice on a chow diet. Mice were injected with insulin (0.75 IU/kg, i.p.), and blood glucose was subsequently measured at the indicated time points ($n = 10–11$, $P > 0.05$). (*D*) Immunoblot of in vivo insulin-stimulated adipose tissue, muscle, and liver. Twenty-one-week-old mice fed a chow diet were starved overnight and anesthetized, followed by i.p. injection of saline or 150 mU/g body weight insulin. After 15 min adipose tissue, muscle and liver were removed and snap frozen. Lysates were run on an SDS-PAGE and immunoblotted for phosphorylated and total Akt, and phosphorylated and total GSK3. (*E*) Basal and insulin-stimulated glucose uptake was measured on isolated adipocytes from *rictor*$^{fl/fl}$ and *rictor*$^{ad-/-}$ mice on a chow diet. Glucose uptake was normalized to cell number, and data are shown in arbitrary units ($n = 5$).

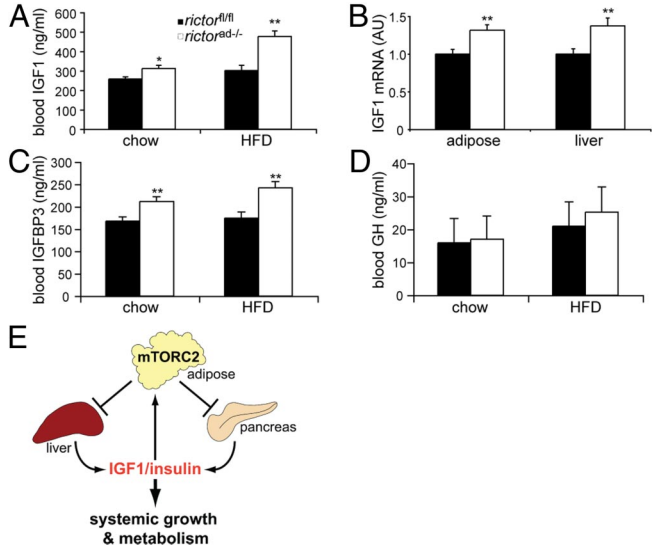

Fig. 6. *Rictor*$^{ad-/-}$ mice have elevated levels of IGF1. (*A*) Blood IGF1 levels in mice fed a chow diet or HFD for 10 weeks. (*B*) IGF1 mRNA expression in adipose tissue (epididymal) and liver of mice fed a chow diet was determined by quantitative RT-PCR. IGF1 expression was normalized to Polr2a expression and is shown in arbitrary units (AU). (*C* and *D*) IGFBP3 (*C*) and GH (*D*) levels were determined in mice fed a chow diet or HFD for 10 weeks. Values in *A–D* are represented as mean ± SEM. *$P < 0.05$; **$P < 0.01$, rictor$^{ad-/-}$ vs. rictor$^{fl/fl}$ ($n = 8–10$). (*E*) Model of adipose mTORC2 regulating whole-body growth. Adipose mTORC2 negatively regulates IGF1 and insulin production by liver and pancreas, respectively, and thereby controls systemic growth and metabolism.

is produced in the pituitary gland and acts by stimulating IGF1 production in the liver. To understand further the increased body size of *rictor*$^{ad-/-}$ mice, we measured serum levels of GH and IGF1. IGF1 serum levels were significantly increased in *rictor*$^{ad-/-}$ mice compared with control *rictor*$^{fl/fl}$ mice, on either a chow (21%) or high-fat diet (58%) (Fig. 6*A*). The increase in IGF1 levels correlated with an increase in IGF1 mRNA levels in the liver, the main IGF1 secreting organ, and in adipose tissue (Fig. 6*B*). In parallel, IGF1 binding protein 3 (IGFBP3) serum levels were also elevated in *rictor*$^{ad-/-}$ mice, on a chow or high-fat diet (26% and 39%, respectively) (Fig. 6*C*). IGFBP3 is the major IGF1 binding protein that together with acid-labile subunit (ALS) stabilizes IGF1 in the serum (29, 30). In contrast, GH serum levels were unchanged (Fig. 6*D*), suggesting that elevated levels of IGF1 in the blood were not due to altered, GH-mediated signaling from the pituitary gland. The increased levels of IGF1 likely account for the increased body size and furthermore contribute to the glucose tolerance of *rictor*$^{ad-/-}$ mice.

Discussion

Here we describe the generation and characterization of mice lacking rictor specifically in adipose tissue. Rictor is an essential and specific subunit of mTORC2. The most striking and unexpected observation was that *rictor*$^{ad-/-}$ mice are increased in body size due to an increase in size of nonadipose tissue. Furthermore, *rictor*$^{ad-/-}$ mice have elevated levels of IGF1 and insulin. The hyperinsulinemia is likely due to a disproportionately increased pancreas and increased β-cell mass. The increase in IGF1 levels is due to a GH-independent increase in IGF1 expression in adipose tissue and the liver. Overall, our findings suggest that mTORC2 in adipose tissue controls an adipose to pancreas/liver signaling axis that ultimately controls whole-body growth and glucose metabolism.

How might mTORC2 in adipose control the pancreas and liver? mTORC2 in adipose tissue may positively control expression and/or secretion of a factor(s) that negatively regulates these organs. Alternatively, adipose mTORC2 could negatively control a factor(s) that positively regulates the pancreas and/or liver. In either case, adipose mTORC2 would negatively regulate the pancreas and liver such that a knockout of adipose mTORC2 results in increased insulin production by the pancreas and increased IGF1 secretion by the liver (Fig. 6*E*). The physiological significance of this negative regulation of the pancreas and liver by adipose mTORC2 may be related to the fact that mTORC2 is itself stimulated by insulin and IGF1 (1). Insulin/IGF1-responsive mTORC2 in adipose tissue may be part of a negative feedback endocrine loop acting on the pancreas and liver to maintain insulin and IGF1 homeostasis (Fig. 6*E*). Consistent with such a negative feedback loop, an adipose-specific knockout of IGF1 receptor results in elevated levels of IGF1 and larger mice but unchanged levels of GH (31), similar to the adipose-specific mTORC2 knockout described here. Thus, according to this model, insulin and IGF1 activate mTORC2 in adipose tissue and this, in turn, leads to downregulation of insulin and IGF1 production in the pancreas and liver, respectively. It will be of interest to determine if disruption of this putative feedback loop between organs plays a role in metabolic or growth disorders. In this context, it is relevant to note that the feedback loop appears to be particularly important in response to a high-fat diet, as suggested by our observation that the growth phenotype of *rictor*$^{ad-/-}$ mice is more pronounced on a high-fat diet.

What is the mTORC2-regulated factor(s) that could be signaling from adipose tissue to the pancreas and/or liver? It must be something other than leptin, IL-6, or free fatty acids as these factors are unchanged in *rictor*$^{ad-/-}$ mice (Table 1). *IGF1* expression is increased in adipose tissue in *rictor*$^{ad-/-}$ mice, suggesting that IGF1 could be a factor by which adipose mTORC2 signals to other organs. However, IGF1 produced by adipose tissue would likely not be a major factor in signaling to the pancreas and liver because there are few to no IGF1 receptors in the liver, and because the liver is the major producer of circulating IGF1. The secreted factor(s) that signals from adipose to the pancreas and liver remains to be determined.

The downstream effectors of mTORC2 that mediate the effects described here are unknown. mTORC2 controls many AGC family kinases (11, 32), and we have shown that an mTORC2 deficiency in adipose tissue results in reduced Akt Ser-473 phosphorylation and reduced levels of PKCα. It seems unlikely that the phenotype described here is due to loss of Akt Ser-473 phosphorylation as loss of Akt Ser-473 phosphorylation only mildly affects Akt activity. PKCα is poorly characterized in adipose tissue, and thus it remains to be determined whether loss of PKCα plays a significant role. Recent findings suggest that the TORC2 substrate and AGC kinase SGK1 plays an important role in TORC2 downstream signaling and thus possibly in the phenotype described here (15, 33, 34). However, SGK1 also remains to be characterized in adipose tissue.

In summary, our findings and the recent findings of Klöting et al. (31) suggest that adipose tissue, and in particular IGF1-mTOR signaling in adipose tissue, plays an unexpectedly central role in controlling whole-body growth. This notion is further supported by Colombani et al. (24) who demonstrated that TOR in the fly fat body controls whole-body growth via a hormonal mechanism. However, mice and flies do not appear to be completely analogous, as adipose mTORC1 in mice does not control systemic growth positively, as suggested for flies (19). In mice, adipose mTORC2 controls systemic growth negatively.

Methods

Mice. *LoxP* sites were introduced into the intron upstream of exon 4 and into the intron downstream of exon 5 using a *neo* cassette flanked with *frt* sites as a selectable marker (Fig. 1*A*). Expression of Cre recombinase deletes exons 4 and 5 and causes a frame shift in the *rictor* ORF. The vector containing the targeting construct was introduced into embryonic stem cells of the129S1/SvlmJ mouse strain, and positive ES cells were selected by G418 resistance. Targeted stem cells were injected into blastocysts of C57BL/6J mice to obtain chimeric mice. Injection

of ES cells into blastocysts and subsequent generation of chimeric mice was performed at the Institut Clinique de la Souris (ICS), Strasbourg, France. After germline transmission, mice were crossed with C57BL/6J mice expressing Flp recombinase to remove the *neo* cassette and subsequently with C57BL/6J Flp deleter mice to obtain *rictor*$^{fl/fl}$mice. The *rictor*$^{fl/fl}$ mice lack the *neo* cassette and behave like wild type. Mice with an adipose-specific deletion of rictor (*rictor*$^{ad-/-}$) were obtained by crossing *rictor*$^{fl/fl}$ mice with C57BL/6J mice expressing Cre recombinase under the control of the adipocyte-specific *fabp4/aP2* gene promoter (25) (purchased from JAX Laboratories), which is expressed relatively late in adipogenesis (35), leading to knockout of *rictor* only in mature adipocytes in neonates. *Rictor*$^{ad-/-}$ mice were born at the expected Mendelian ratio. For all experiments, male mice that had been backcrossed at least 5 times with the C57BL/6 strain were used. Littermates with the *lox/lox* genotype (*rictor*$^{fl/fl}$) were used as control group in all experiments and are indistinguishable from wild-type mice. All mouse experiments described were approved by the Kantonales Veterinaeramt of Kanton Basel-Stadt.

Metabolic Studies. At 8 weeks of age, male mice were fed either a normal chow diet (4.5% calories from fat; Kliba Nafag) or a high-fat diet (60% calories from fat; Harlan Research Diets) and monitored for 10 weeks. Body weight was recorded weekly. Quantification of blood metabolites was performed using commercially available kits.

Dual-Energy X-ray Absorptiometry (Dexa) Scan Analysis. Dexa scan analysis was performed with the ultra-high-resolution densitometer PIXImus (GE Medical Systems), allowing precise measurement of bone density and body composition (fat and lean mass). Bone mineral content and density and body composition were recorded on anesthetized mice.

Histological Analysis. Liver tissues were prepared for cryosectioning, and sections were stained with Oil Red O and hematoxylin. Pancreas and adipose tissue were fixed in 4% formaldehyde and paraffin embedded using a standard protocol. Adipose tissue sections were prepared and stained with hematoxylin and eosin (H&E). For islet size quantification, pancreatic sections (8 μm) were cut in regular intervals, and sequential sections were stained with H&E. All sections were photographed, and the area of every islet was quantified using ImageJ software. On average, 40 islets per pancreas were analyzed. For quantification of β-cell mass, β cells were stained using rabbit antibodies against insulin and detected with a secondary antibody conjugated with horseradish peroxidase (Vectastain ABC Kit; Vector Labs) followed by incubation in DAB peroxidase substrate solution and subsequent counterstaining with hematoxylin. Images of the entire pancreatic section were obtained using a digital microscope (Coolscope; Nikon), and sections were analyzed using ImageJ software. The β-cell mass was calculated by the percentage of β-cell area and pancreas weight. For immunofluorescence, pancreatic sections were stained for insulin and glucagon using rabbit antibodies against insulin and mouse antibodies against glucagon. Immune complexes were detected with secondary antibodies conjugated with Texas Red or FITC, respectively.

Glucose Uptake into Adipocytes. Adipocytes were isolated from epididymal and inguinal fat pads by 60-min digestion in KRBH buffer containing 1% BSA and 1,100 U/mL collagenase. Cells were starved for an additional 60 min in KRBH buffer containing 1% BSA. During the last 30 min, 100 nM insulin was added. To measure glucose uptake, isolated adipocytes were washed once in HBS buffer (140 mM NaCl, 20 mM Hepes [pH 7.4], 5 mM KCl, 2.5 mM $MgSO_4$, 1 mM $CaCl_2$) and incubated for 10′ in transport solution (HBS containing 10 μM 2-deoxy glucose and 0.5 uCi/mL ^{3}H 2-deoxy glucose). Cells were washed 3 times in cold PBS, and radioactivity was measured by scintillation counter. Glucose uptake was normalized to cell number, which was determined by qPCR on intronic DNA. Primers used were 5′-CTACAGATGTGGTAAAGGTCCGC-3′ and 5′-GCAATGGTCTTGTAGGCTTCG-3′.

Quantitative PCR. Total RNA was isolated from frozen tissues using TriZOL reagent (Invitrogen). Three micrograms total RNA was reverse transcribed using SuperScript II reverse transcriptase (Invitrogen) and random nonamers. qPCR was performed using the Power SYBR Green Mix (Applied Biosystems) and normalized to Polr2a expression. The following primers were used: Polr2a sense 5′-AATCCGCATCATGAACAGTG-3′, Polr2a antisense 5′-CAGCATGTTGGACTCAATGC-3′, IGF1 sense 5′-GCTGCTGAAGCCATTCATTT-3′, and IGF1 antisense 5′-TTGCTCTTAAGGAGGCCAAA-3′.

Statistical Analysis. All data are shown as mean ± SEM. Statistical significance between 2 groups was determined using unpaired, two-tailed Student's *t* test. $*P < 0.05$; $**P < 0.01$.

ACKNOWLEDGMENTS. We thank A. Hein, K. Beier, I. Ginez, W. Dolci, and A. Löschmann for technical assistance, and T. Sorg, X. Warot, and M.F. Champy for support in generation and phenotyping of knockout mice. We acknowledge support from the Roche Research Foundation (P.P.), the Swiss National Science Foundation, and the Canton of Basel (M.A.R. and M.N.H.).

1. Wullschleger S, Loewith R, Hall MN (2006) TOR signaling in growth and metabolism. *Cell* 124(3):471–484.
2. Haar EV, Lee S-i, Bandhakavi S, Griffin TJ, Kim D-H (2007) Insulin signalling to mTOR mediated by the Akt/PKB substrate PRAS40. *Nat Cell Biol* 9(3):316–323.
3. Hara K, et al. (2002) Raptor, a binding partner of target of rapamycin (TOR), mediates TOR action. *Cell* 110(2):177–189.
4. Kim DH, et al. (2002) mTOR interacts with raptor to form a nutrient-sensitive complex that signals to the cell growth machinery. *Cell* 110(2):163–175.
5. Loewith R, et al. (2002) Two TOR complexes, only one of which is rapamycin sensitive, have distinct roles in cell growth control. *Mol Cell* 10(3):457–468.
6. Jacinto E, et al. (2006) SIN1/MIP1 maintains rictor-mTOR complex integrity and regulates Akt phosphorylation and substrate specificity. *Cell* 127(1):125–137.
7. Jacinto E, et al. (2004) Mammalian TOR complex 2 controls the actin cytoskeleton and is rapamycin insensitive. *Nat Cell Biol* 6(11):1122–1128.
8. Sarbassov DD, et al. (2004) Rictor, a novel binding partner of mTOR, defines a rapamycin-insensitive and raptor-independent pathway that regulates the cytoskeleton. *Curr Biol* 14(14):1296–1302.
9. Sarbassov DD, et al. (2006) Prolonged rapamycin treatment inhibits mTORC2 assembly and Akt/PKB. *Mol Cell* 22(2):159–168.
10. Yang Q, Inoki K, Ikenoue T, Guan K-L (2006) Identification of Sin1 as an essential TORC2 component required for complex formation and kinase activity. *Genes Dev* 20(20):2820–2832.
11. Polak P, Hall MN (2009) mTOR and the control of whole body metabolism. *Curr Opin Cell Biol* 21:209–218.
12. Hresko RC, Mueckler M (2005) mTOR·RICTOR is the Ser473 kinase for Akt/protein kinase B in 3T3–L1 adipocytes. *J Biol Chem* 280(49):40406–40416.
13. Sarbassov DD, Guertin DA, Ali SM, Sabatini DM (2005) Phosphorylation and regulation of Akt/PKB by the rictor-mTOR complex. *Science* 307(5712):1098–1101.
14. Facchinetti V, et al. (2008) The mammalian target of rapamycin complex 2 controls folding and stability of Akt and protein kinase C. *EMBO J* 27(14):1932–1943.
15. Garcia-Martinez JM, Alessi DR (2008) mTOR complex-2 (mTORC2) controls hydrophobic motif phosphorylation and activation of serum and glucocorticoid induced protein kinase-1 (SGK1). *Biochem J* 416:375–385.
16. Ikenoue T, Inoki K, Yang Q, Zhou X, Guan KL (2008) Essential function of TORC2 in PKC and Akt turn motif phosphorylation, maturation and signalling. *EMBO J* 27(14):1919–1931.
17. Guertin DA, et al. (2006) Ablation in mice of the mTORC components raptor, rictor, or mLST8 reveals that mTORC2 is required for signaling to Akt-FOXO and PKCα, but not S6K1. *Dev Cell* 11(6):859–871.
18. Shiota C, Woo J-T, Lindner J, Shelton KD, Magnuson MA (2006) Multiallelic disruption of the rictor gene in mice reveals that mTOR complex 2 is essential for fetal growth and viability. *Dev Cell* 11(4):583–589.
19. Polak P, et al. (2008) Adipose-specific knockout of raptor results in lean mice with enhanced mitochondrial respiration. *Cell Metab* 8(5):399–410.
20. Bentzinger CF, et al. (2008) Skeletal muscle-specific ablation of raptor, but not of rictor, causes metabolic changes and results in muscle dystrophy. *Cell Metab* 8(5):411–424.
21. Kumar A, et al. (2008) Muscle-specific deletion of rictor impairs insulin-stimulated glucose transport and enhances basal glycogen synthase activity. *Mol Cell Biol* 28(1):61–70.
22. Haugen F, Drevon CA (2007) The interplay between nutrients and the adipose tissue. *Proc Nutr Soc* 66(2):171–182.
23. Shi Y, Burn P (2004) Lipid metabolic enzymes: Emerging drug targets for the treatment of obesity. *Nat Rev Drug Discov* 3(8):695–710.
24. Colombani J, et al. (2003) A nutrient sensor mechanism controls drosophila growth. *Cell* 114(6):739–749.
25. He W, et al. (2003) Adipose-specific peroxisome proliferator-activated receptor gamma knockout causes insulin resistance in fat and liver but not in muscle. *Proc Natl Acad Sci USA* 100(26):15712–15717.
26. Liao L, et al. (2006) Liver-specific overexpression of the insulin-like growth factor-i enhances somatic growth and partially prevents the effects of growth hormone deficiency. *Endocrinology* 147(8):3877–3888.
27. Butler AA, Roith DL (2001) Control of growth by the somatropic axis: Growth hormone and the insulin-like growth factors have related and independent roles. *Annu Rev Physiol* 63(1):141–164.
28. Dupont J, Holzenberger M (2003) Biology of insulin-like growth factors in development. *Birth Defects Research Part C: Embryo Today: Reviews* 69(4):257–271.
29. Yakar S, et al. (2005) Metabolic effects of IGF-I deficiency: Lessons from mouse models. *Pediatr Endocrinol Rev* 3(1):11–19.
30. Duan C, Xu Q (2005) Roles of insulin-like growth factor (IGF) binding proteins in regulating IGF actions. *Gen Comp Endocrinol* 142(1–2):44–52.
31. Klöting N, et al. (2008) Autocrine IGF-1 action in adipocytes controls systemic IGF-1 concentrations and growth. *Diabetes* 57:2074–2082.
32. Jacinto E, Lorberg A (2008) TOR regulation of AGC kinases in yeast and mammals. *Biochem J* 410(1):19–37.
33. Jones KT, Greer ER, Pearce D, Ashrafi K (2009) Rictor/TORC2 regulates Caenorhabditis elegans fat storage, body size, and development through sgk-1. *PLoS Biol* 7(3):e60.
34. Soukas AA, Kane EA, Carr CE, Melo JA, Ruvkun G (2009) Rictor/TORC2 regulates fat metabolism, feeding, growth, and life span in Caenorhabditis elegans. *Genes Dev* 23(4):496–511.
35. Tontonoz P, Hu E, Spiegelman BM (1994) Stimulation of adipogenesis in fibroblasts by PPARγ2, a lipid-activated transcription factor. *Cell* 79(7):1147–1156.